Hindawi Publishing Corporation
Mathematical Problems in Engineering
Volume 2015, Article ID 630135, 9 pages
http://dx.doi.org/10.1155/2015/630135

Research Article

Nonlinear Dynamic Analysis of Railway Wagon End Wall under the Action of Granular Media

Jing Wang,[1] Qichang Zhang,[1] Yuebin Yu,[2] Jianxin Han,[1] and Dong Li[3]

[1]*School of Mechanical Engineering, Tianjin University, Tianjin 300072, China*
[2]*Qiqihar Railway Rolling Stock Co., Ltd., Qiqihar 161992, China*
[3]*Tianjin Key Laboratory of High Speed Cutting and Precision Machining, Tianjin University of Technology and Education, Tianjin 300222, China*

Correspondence should be addressed to Yuebin Yu; yuebinyu2015@163.com

Received 12 May 2015; Accepted 27 July 2015

Academic Editor: John D. Clayton

In wagon end wall system under the action of granular media, the model of the wall is the result of multiple factors. To figure out how the key factors act, the large amplitude vibration together with the contribution from the action of granular media to build the nonlinear dynamics equation of the wagon end wall has been taken into account. In this paper, the effects of varying damping, added mass, and force due to the action of granular media on the patterns of movement and response performance were discussed in detail. Furthermore, the finite element model of end wall-granular media was established. It proves that the theoretical result is correct compared with the FEM results. It indicates that the resonance frequency of the wall declines with the increase of the height of granular media, while the frequency increases with the increase of the particle size of granular media. The nonlinear dynamics of the wall is less affected by the height ratio and particle size of granular media, while it is greatly affected by the height and the thickness of wall, which should be seriously considered in structural design of the wagon.

1. Introduction

70% of the total railway freight transportation is with granular media loaded in, such as coal and rubble. Research on dynamics of the wagon is acknowledged difficult for the special stress-strain relationship, development of strength and deformation, and response of nonlinear dynamic and complicated coupling property of granular media.

With the rapid development of high-speed and heavy-loading trains, the security of the railroad running becomes more and more important. Thus, it is essential to design some new types of heavy haul freight cars. However, as the car speed increases, the intensity of excitation and the frequency variation increase. Then, wagon will show a complex dynamic response under the action of granular media, so the deformation of bending and torsion will increase and the probability of local damage will also increase. The mechanical properties increase the difficulty of the design and limit the development of cars. So, it is significantly meaningful to investigate the nonlinear dynamics of the bulk carrier.

A group of international and domestic academics launched a series of research on mechanics of granular media [1] and related area. In Guaita et al.'s works [2], an elastoplastic constitutive law was applied to cylindrical silos with eccentric hoppers and rigid walls, using the Drucker-Prager criterion. Meng et al. [3] dealt with the application of a secant constitutive relationship for bulk solids in a transient finite element analysis of stresses, displacements, and velocities during discharge of soybean from a silo. Goodey et al. [4] outlined the development and verification of a finite element model for the filling pressure distribution in a square platform silo with flexible walls. Ayuga et al. [5] used FEM models to represent the various problems in silo analysis and the influence of different parameters was discussed. Zhang et al. [6] studied the mechanical behavior of granular media in a wagon by discrete element method (DEM). The mechanical behavior of granular media was studied in different conditions by He et al. [7] and they drew the conclusion that lateral static pressure is under linear distribution along height division of wagon.

However, the above works lacked studies on dynamics of the bulk carrier, and their theories do not perform very well when applied to wagon end wall system, since they fail to consider the coupling relationship between granular media and bulk carrier. Several researches on dynamic behavior of soil-wall systems were carried out. To represent the unbounded half-space soil in a soil-structure interaction analysis, Wolf and Somaini [8] used a discrete model that consists of a mass which is attached to a rigid support with a spring and a damper. Ghanbari et al.'s formula [9] considered the vertical cross-sectional width change, thus calculating the natural frequency of retaining walls. As the increase of width to length ratio, the frequency of wall decreases. Hatami and Bathurst [10] discussed the effect of fundamental frequency of reinforced-soil retaining walls on the influence of some design parameters including wall height, backfill width, reinforcement stiffness, reinforcement length, backfill friction angle, and toe restraint condition. But there are few researches focusing on wagon end wall. The coupling relationship could be measured by resonant frequency and amplitude-frequency response of system, and these parameters will significantly influence the performance of the wagon end wall. To fill this research gap, this paper proposes using theoretical and FEM method based on geotechnical mechanics to study the relationship between the key structural designing parameter and the dynamic response of the wagon end wall after high-speed and heavy-loading trains are loaded with granular media. The numerical study results clearly show the influences of the key structural designing parameters on the dynamic response of the wagon end wall and demonstrate our conclusions. This paper provides a foundation for the design of the wagon and the structural optimization and improves the effect of working performance.

2. Theoretical Analysis

2.1. The Derivation Process of Added Mass about Wagon End Wall. We first need to consider the added mass caused by granular media when computing the dynamic characteristics of wall contact with granular media. Because the nature of granular media lies between solid and fluid, it has complicated mechanics characteristics, though the particle is of simple structure.

A semiempirical formula was introduced according to the results of experiment and the empirical derivation [11]. The wall was regarded as a pile with a diameter of a. The added mass of the whole pile is

$$\begin{aligned} M_{a0} &= \rho_a \left[\frac{\pi}{27} \left(r^2 b_a + 16 r^3 \right) - \frac{b_a}{9} A \right] \\ &= \rho_a \left[\frac{\pi}{27} \left(r^2 b_a + 16 r^3 \right) - \frac{b_a \pi a^2}{36} \right], \end{aligned} \tag{1}$$

where $r = (1/2)((2/3)L \tan(\varphi/2) + d)$ is the diffusion radius, φ is the friction angle, and b_a is the height of granular media.

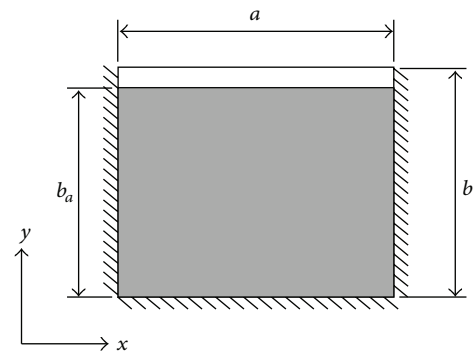

Figure 1: Model of the rectangular plate with three clamped edges and a free edge.

Distribution of added mass was simplified into triangular distribution. The added mass on the top was 0, so the total added mass per unit area is

$$\begin{aligned} M &= M_0 + M_a \\ &= h\rho + \frac{2(b_a - y)}{h b_a^{\,2}} \rho_a \pi \left[\frac{1}{27} \left(r^2 b_a + 16 r^3 \right) - \frac{a^2 b_a}{36} \right], \end{aligned} \tag{2}$$

where ρ is the density of the wall, ρ_a is the density of granular media, and M_0 is the mass of the wall per unit area. M_a is the added mass per unit area.

2.2. The Establishment of Dynamics Equation. The dynamical model of the wagon end wall was simplified as a plate with one free edge on the top and three other fixed edges. This model has a good performance on the dynamic characteristic of the system and can describe it accurately, as shown in Figure 1. a is the width of the wall, b is the height of the wall, h is the thickness of the wall, and b_a is the height of granular media. The nonlinear dynamic equation of a wall is derived based on Von Karman theory, with the added mass and damping effect taken into account:

$$\begin{aligned} &D \left(\frac{\partial^4 w}{\partial x^4} + 2 \frac{\partial^4 w}{\partial x^2 \partial y^2} + \frac{\partial^4 w}{\partial y^4} \right) + c \frac{\partial w}{\partial t} + M \frac{\partial^2 w}{\partial t^2} + v \\ &\quad = p(x, y, t), \end{aligned} \tag{3}$$

where $v = -\{(Eh/2(1-\mu^2))(\partial^2 w/\partial x^2)[(\partial w/\partial x)^2 + \mu(\partial w/\partial y)^2] + (Eh/2(1-\mu^2))(\partial^2 w/\partial y^2)[(\partial w/\partial y)^2 + \mu(\partial w/\partial x)^2] + (Eh/(1+\mu))(\partial w/\partial x)(\partial w/\partial y)(\partial^2 w/\partial x \partial y)\}$, in which w is the deflection of the wall, E is the elasticity modulus of the wall, μ is Poisson's ratio of the wall, ρ is the density of the wall, $D = Eh^3/12(1-\mu^2)$ is the bending rigidity of the wall, and c is the damping coefficient.

The pressure [12] of granular media to the wall can be described by

$$p(x, y, t) = p_0 + p_1 \sin \omega t, \tag{4}$$

where p_0 is the static lateral pressure of the wall, p_1 is the pressure amplitude of vibration provided by granular media, and ω is the vibration frequency of granular media.

According to Coulomb's earth pressure theory, the lateral pressure of the wall is

$$p_0 = K\left[\left(-\frac{\gamma b}{\alpha K-2}\right)\left(\frac{b-y}{b}\right)^{\alpha K-1}+\frac{\gamma(b-y)}{\alpha K-2}\right], \quad (5)$$

where $K = \cos\theta\cos\delta\sin(\theta-\varphi)/\sin\theta\cos(\theta-\varphi+\delta)$, $\alpha = \cos(\theta-\varphi-\delta)\tan\theta/\sin(\theta-\varphi)\cos\delta$, K is the lateral pressure coefficient of granular media, θ is the angle between slip surface and horizontal surface, φ is the internal friction angle of granular media, δ is the angle of friction between the wall and granular media, and γ is the force density of granular media.

Based on first-order modal of out-of-plane vibration, the vibration model functions can be written as

$$w(x,y,t) = W(x,y)\varphi(t) = X(x)Y(y)\varphi(t). \quad (6)$$

The plate is with one free end on the top and three other fixed edges, so the boundary condition is as follows:

free end:

$$M_y\big|_{y=0} = V_y\big|_{y=0} = 0; \quad (7)$$

that is,

$$\left(\frac{\partial^2 w}{\partial y^2}+\mu\frac{\partial^2 w}{\partial x^2}\right)\Bigg|_{y=0} = 0,$$
$$\left[\frac{\partial^3 w}{\partial y^3}+(2-\mu)\frac{\partial^3 w}{\partial x^2\partial y}\right]\Bigg|_{y=0} = 0; \quad (8)$$

fixed edges:

$$w|_{x=0} = w|_{x=a} = w|_{y=b} = 0; \quad (9)$$

that is,

$$\left.\frac{\partial w}{\partial x}\right|_{x=0} = \left.\frac{\partial w}{\partial x}\right|_{x=a} = \left.\frac{\partial w}{\partial y}\right|_{y=b} = 0. \quad (10)$$

Given the vibration model function [13] as $W(x,y) = (\cos(2\pi x/a)-1)(1-\cos(\pi y/2b))$, then (6) can be described as

$$w(x,y,t) = \left(\cos\frac{2\pi x}{a}-1\right)\left(1-\cos\frac{\pi y}{2b}\right)\cdot\varphi(t). \quad (11)$$

Substituting (11) into (3), the residual can be obtained by Galerkin method

$$R = \nabla^4 W(x,y)\varphi(t)+\frac{1}{D}V(x,y)\varphi^3(t) + \frac{c}{D}W(x,y)\varphi'(t)+\frac{M}{D}W(x,y)\varphi''(t) - \frac{p_0+p_1\sin\Omega t}{D} \quad (12)$$

because

$$\int_0^a\int_0^b RW_{ij}(x,y)\,dx\,dy = 0. \quad (13)$$

Substituting (12) into (13), it can be obtained that

$$\varphi''(t)+\frac{a_2}{a_1}\varphi'(t)+\frac{a_3}{a_1}\varphi(t)+\frac{a_4}{a_1}\varphi^3(t) = \frac{a_5}{a_1}+\frac{a_6}{a_1}\sin\Omega t, \quad (14)$$

where

$$a_1 = \frac{M}{D}\int_0^a\int_0^b W^2(x,y)\,dx\,dy,$$
$$a_2 = \frac{c}{D}\int_0^a\int_0^b W^2(x,y)\,dx\,dy,$$
$$a_3 = \int_0^a\int_0^b W(x,y)\nabla^4 W(x,y)\,dx\,dy,$$
$$a_4 = \frac{1}{D}\int_0^a\int_0^b V(x,y)W(x,y)\,dx\,dy,$$
$$a_5 = \frac{1}{D}\int_0^a\int_0^{b_a} W(x,y)p_0\,dx\,dy,$$
$$a_6 = \frac{p_1}{D}\int_0^a\int_0^b W(x,y)\,dx\,dy. \quad (15)$$

For convenience, introduce the following nondimensional variables:

$$\frac{a_3}{a_1} = {\omega_0}^2,$$
$$\Psi = \frac{\varphi}{h},$$
$$\tau = \omega_0 t. \quad (16)$$

Consider $\psi = u+\varphi_0$; then the equation of vibration becomes

$$u''+u = \varepsilon\left[c_1\sin\frac{\Omega\tau}{\omega_0}+c_2u'+c_3u^3+3c_3\varphi_0u^2+3c_3\varphi_0^2u\right], \quad (17)$$

where

$$c_1 = \frac{a_6}{a_1}\frac{1}{h{\omega_0}^2}p_1,$$
$$c_2 = -\frac{a_2}{a_1}\frac{1}{\omega_0},$$
$$c_3 = -\frac{a_4}{a_1}h^2\frac{1}{{\omega_0}^2}. \quad (18)$$

2.3. Perturbation Solution. The method of multiple scale is used to investigate the dynamic behavior of (17) under the primary resonance condition; namely, $\Omega/\omega_0 \approx 1$.

To describe the nearness of the primary resonance condition, a detuning parameter σ is introduced and defined by

$$\frac{\Omega}{\omega_0} = 1 + \varepsilon\sigma. \tag{19}$$

Introduce time-scale $T_n = \varepsilon^n t$, $n = 0, 1, 2, \ldots$; then the approximate solution of (17) can be written as

$$u(t) = u_0(T_0, T_1) + \varepsilon u_1(T_0, T_1). \tag{20}$$

Substituting (19) and (20) into (17) and equating the coefficients of ε^0 and ε^1 on both sides, we can obtain

$$D_0^2 u_0 + u_0 = 0, \tag{21}$$

$$\begin{aligned} D_0^2 u_1 + u_1 = {} & -2D_0 D_1 u_0 + c_1 \sin(T_0 + \varepsilon\sigma T_0) \\ & + c_2 D_0 u_0 + c_3 u_0^3 + 3c_3\varphi_0 u_0^2 \\ & + 3c_3\varphi_0^2 u_0, \end{aligned} \tag{22}$$

where $D_n = \partial/\partial T_n$, $n = 0, 1$.

The solution of (21) is given in the form

$$u_0 = A(T_1) e^{iT_0} + \overline{A}(T_1) e^{-iT_0}; \tag{23}$$

then (22) becomes

$$\begin{aligned} {D_0}^2 u_1 + u_1 = {} & e^{iT_0}\left(-2iD_1 A + \frac{c_1}{2i} e^{i\sigma T_1} + c_2 iA \right. \\ & \left. + 3c_3 A^2\overline{A} + 3c_3\varphi_0^2 A\right) + c_3 A^3 e^{3iT_0} + 3c_3\varphi_0 A^2 e^{2iT_0} \\ & + 3c_3\varphi_0 A\overline{A} + \text{cc}, \end{aligned} \tag{24}$$

where cc denotes the complex conjugate of the preceding terms.

To eliminate secular terms, we must put

$$-2iD_1 A + \frac{c_1}{2i} e^{i\sigma T_1} + c_2 iA + 3c_3 A^2\overline{A} + 3c_3\varphi_0^2 A = 0; \tag{25}$$

then

$$\begin{aligned} \frac{\partial^2 u_1}{\partial {T_0}^2} + u_1 = {} & c_3 A^3 e^{3iT_0} + 3c_3\varphi_0 A^2 e^{2iT_0} + 3c_3\varphi_0 A\overline{A} \\ & + \text{cc}. \end{aligned} \tag{26}$$

So we obtain

$$u_1 = -\frac{1}{8} c_3 A^3 e^{3iT_0} - c_3\varphi_0 A^2 e^{2iT_0} + 3c_3\varphi_0 A\overline{A} + \text{cc}. \tag{27}$$

It is convenient to write A in the polar form

$$A(T_1) = \frac{1}{2} a_0(T_1) e^{i\theta(T_1)}. \tag{28}$$

Substituting (28) into (25), we obtain

$$\begin{aligned} \frac{da_0}{dT_1} &= \frac{1}{2} c_2 a_0 - \frac{c_1}{2}\cos\gamma, \\ a_0\frac{d\gamma}{dT_1} &= -a_0\sigma - 3c_3 a_0^3 - \frac{3}{2} c_3\varphi_0^2 a_0 + \frac{c_1}{2}\sin\gamma, \end{aligned} \tag{29}$$

where $\gamma = \theta - \sigma T_1$.

The amplitude-frequency response equation can be obtained as follows by imposing the condition $da_0/dT_1 = d\gamma/dT_1 = 0$:

$$\left(2a_0\sigma + 6c_3 {a_0}^3 + 3c_3 {\varphi_0}^2 a_0\right)^2 + \left(c_2 a_0\right)^2 = {c_1}^2, \tag{30}$$

and the first approximated solution of system can be expressed as

$$\begin{aligned} w(x, y, t) = {} & \left[-\frac{1}{64} c_3 {a_0}^3 (T_1) e^{3i\theta(T_1) + 3iT_0} \right. \\ & \left. - \frac{1}{4} c_3\varphi_0 {a_0}^2 (T_1) e^{2i\theta(T_1) + 2iT_0} + \frac{3}{4} c_3\varphi_0 {a_0}^2 (T_1) + \text{cc}\right] \\ & \cdot h\left(\cos\frac{2\pi x}{a} - 1\right)\left(1 - \cos\frac{\pi y}{2b}\right). \end{aligned} \tag{31}$$

3. Theoretical Analysis

3.1. Resonance Frequency. Resonance frequency is an important design index. The effect of height and particle size of granular media on resonance frequency is discussed in this section.

3.1.1. Effect of Height of Granular Media on Resonance Frequency. The height of granular media directly influences the system vibration. Figure 2 shows that the resonance frequency decreases with the increase of the height of granular media. The added mass increases with the increment of height, which induces the reduction of frequency. At the same time, the lateral pressure on the end wall increases as the granular media increase. It leads to the increment of stiffness and then increment of system frequency. Both factors have an influence together and consequently lead to the reduction of frequency. Furthermore, it should be noted that the added mass plays a greater influence on resonance frequency than the lateral pressure.

3.1.2. Effect of Particle Size of Granular Media on Resonance Frequency. The granular media transported by heavy railway freight car often show different particle sizes, and some typical types of cargoes include coal, ore, wood, steels, and other bulk cargoes. Granular media in different particle size have a direct impact on the vibration of the end wall system. Table 1 shows the density and friction angle of different particle size of gravel. As the particle size increases, density reduces and friction angle increases. And Figure 3 also illustrates that the system frequency increases with the increment of particle size.

Table 1: Parameter table of granular media.

Particle size/(cm)	ρ_a/(kg/m^3)	φ/(°)
0.5	1900	32
0.6	1840	33
0.7	1780	34
0.8	1720	35
0.9	1660	36
1	1600	37
1.1	1540	38
1.2	1480	39
1.3	1420	40
1.4	1360	41
1.5	1300	42

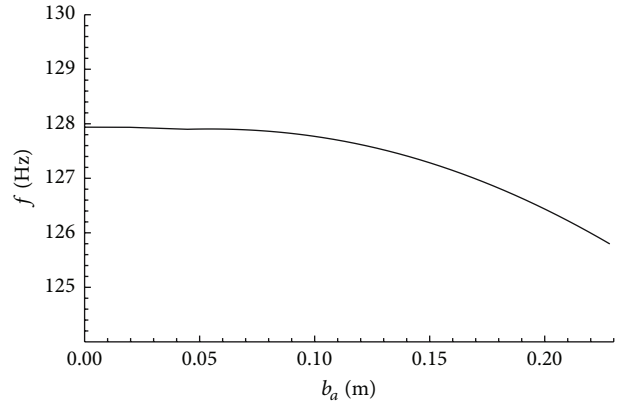

Figure 2: Relationship between resonance frequency and height of granular media.

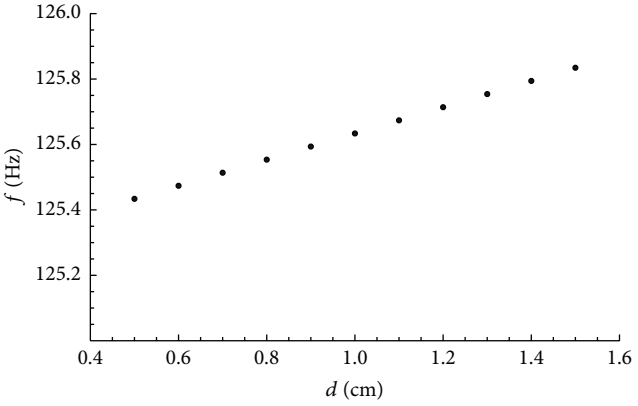

Figure 3: Relationship between resonance frequency and particle size of granular media.

3.2. Amplitude-Frequency Response. Recall the amplitude-frequency response of the end wall in (30). The nonlinear controlling factors include height ratio of granular media, height of the end wall, particle size of granular media, and thickness of the end wall. This section discusses the influence of the above parameters on the vibration characteristics of the system.

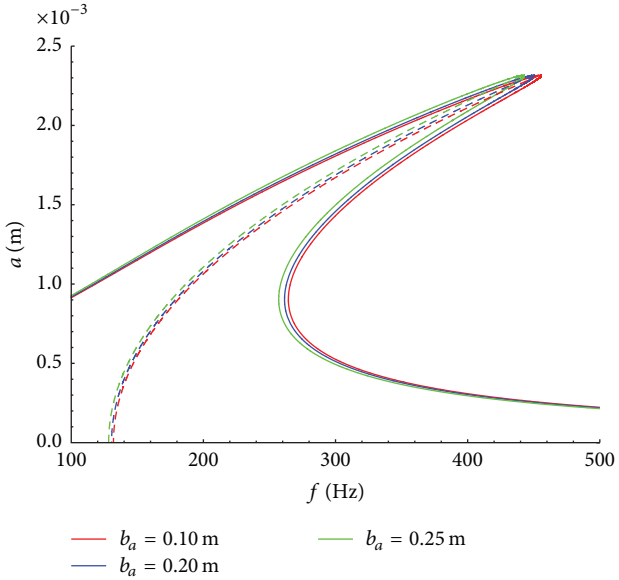

Figure 4: Amplitude-frequency response curve of system under different height ratio of granular media.

3.2.1. Effect of Height Ratio of Granular Media on Amplitude-Frequency Response Curve. Height ratio of granular media is defined as b_a/b. It is used to express the loading capacity. Figure 4 shows the amplitude-frequency response curve for $b_a = 0.1, 0.2, 0.25$; that is, $b_a/b = 2/5, 4/5, 1$, with red, blue, and green curve, respectively. The resonance frequency of the end wall decreases as the height ratio of granular media increases. However, the changing amplitude of the curves is negligibly small, and the stable amplitudes together with the resonance floating excursion are nearly the same. It suggests that the stiffness of the end wall contributed by the interaction between the end wall and granular media on working condition is negligible, and the amount of the granular media has little effect on the nonlinear characteristics of the end wall. Therefore, it is not necessary to consider whether the carriage is in working condition at design time. It will reduce the number of the working conditions to be checked and then light the designing workload.

3.2.2. Effect on Amplitude-Frequency Response Curve by Height of the End Wall. Figure 5 shows the amplitude-frequency response curves when the height of the end wall b = 0.23, 0.25, 0.3 with wagon fully loaded. With the increment of the height of end wall, the nonlinear resonance frequency and the resonance floating excursion of the end wall increase and the nonlinearity becomes stronger. Furthermore, the nonlinearity of structural vibration has the same trend. This indicates that the higher the end wall is, the greater the impact of the granular media on the nonlinear characteristics of the end wall is. So the height-width ratio of the end wall has to be considered during the design of the end wall. Reasonable height-width ratio can reduce the nonlinear vibration of the structure. The height of the carriage should be within a fixed range because the track width is a fixed value in a country. The size of the end wall can be definite if the height-width

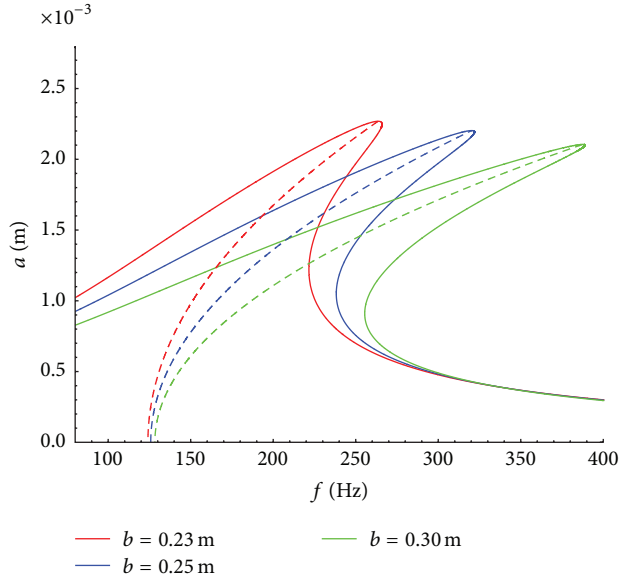

Figure 5: Amplitude-frequency response curve of system under different height of the wall.

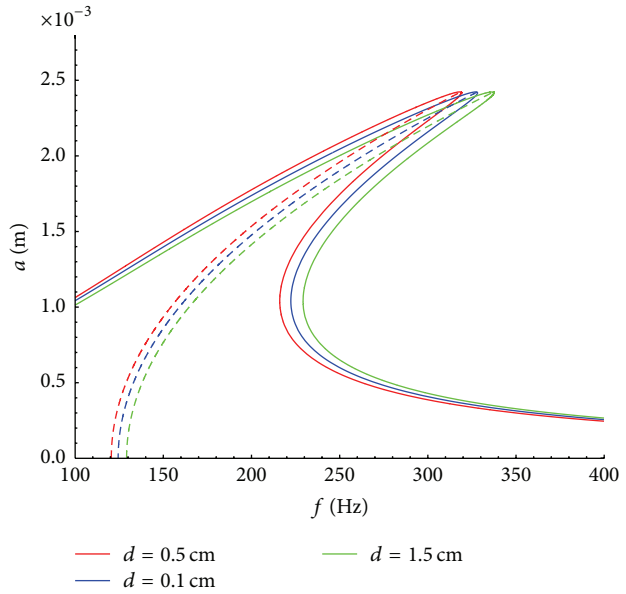

Figure 6: Amplitude-frequency response curve of system under different particle size of granular media.

ratio is known. So, the key point of designing the carriage is to determine the optimal height-width ratio of the carriage.

3.2.3. Effect of Particle Size of Granular Media on Amplitude-Frequency Response. We further discuss the influence of gravel particle size loaded in the carriage on the amplitude-frequency response. Three particle sizes, 0.5 cm, 1 cm, and 1.5 cm, are considered. As shown in Figure 6, the nonlinear resonance frequency of the end wall increases with the increment of the particle size of the granular media. However, the increasing sizes of the curves are quite small and the resonance floating excursion is nearly the same. Therefore we can conclude that the particle size of the granular media has little impact on nonlinear characteristics of structure. The end wall of the carriage has good versatility. The carriage can carry different kinds of cargoes in working condition. So, it does not need to design different carriages for different cargoes. This point can reduce the design workload greatly and has significant implications for the design work.

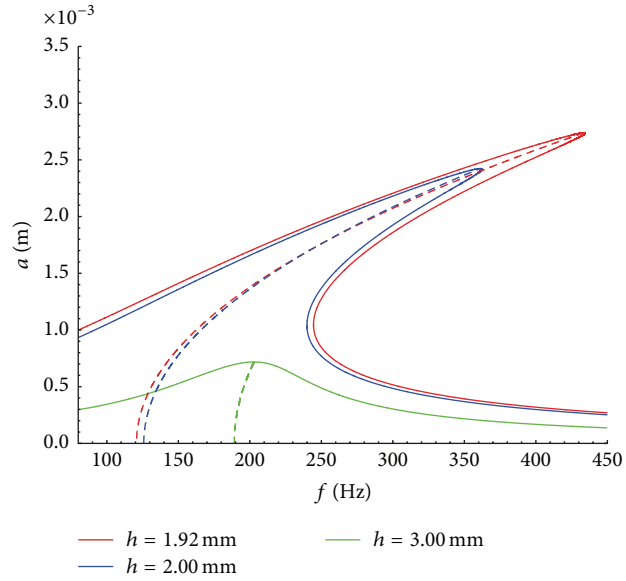

Figure 7: Amplitude-frequency response curve of system under different thickness of the wall.

3.2.4. Effect of Thickness of the End Wall on Amplitude-Frequency Response Curve. The thickness of the end wall is a key parameter in design. Figure 7 shows amplitude-frequency response curve of the system under different thickness, 1.92 mm, 2 mm, and 3 mm, of the wall. It can be seen clearly that the resonance floating excursion decreases greatly as the thickness increases. The resonance floating excursion decreases to nearly 0 when the thickness goes larger than 3 mm. Then, in this case, the end wall shows linear vibration characteristics and steady amplitude-frequency response. It proves that the thickness of end wall can affect the vibration characteristics of the structure. But when the thickness is larger than a specific value, stiffness should be regarded as the key factor which can affect the nonlinear characteristics of the structure instead of thickness. It will reduce the design workload to some extent.

4. Numerical Analysis

This section sets up finite element model to calculate the system for studying the vibration characteristics of the end wall. It validates the rationality of the theory and method above and testifies the correctness of the calculation result.

The key issues to consider are the nonlinear constitutive relation of the granular media, the simulation of contact relationship between granular media and end wall, and

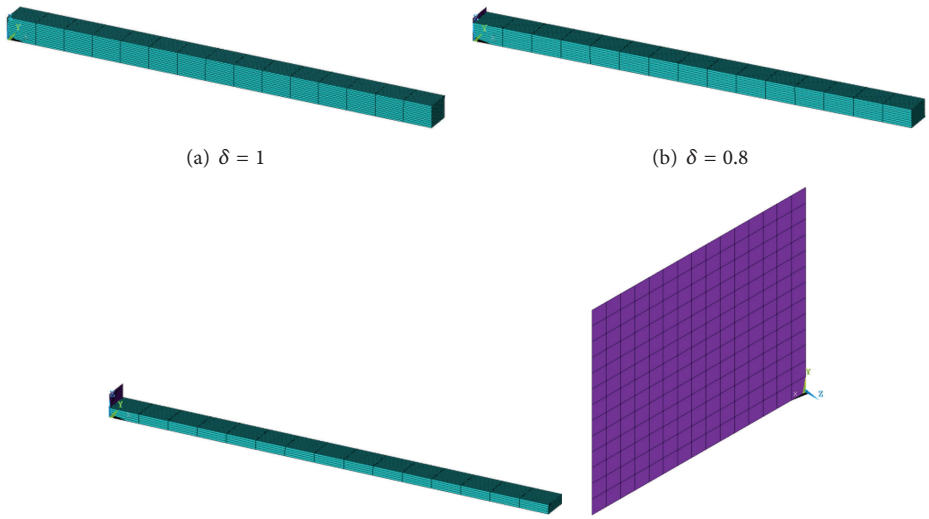

(a) $\delta = 1$ (b) $\delta = 0.8$

(c) $\delta = 0.4$ (d) $\delta = 0$

Figure 8: FEM model of the wall system with different δ.

the simulation of the boundary condition to set up the finite element model of the end wall. We define the height ratio of the granular media $\delta = b_a/b$, by introducing the theory of finite element modeling of the retaining wall structure; we considered the special contact relationship (e.g., see [14–22]) between granular media and continuum and set up finite element models with different δ; the FEM model is shown in Figure 8.

Deformation of granular media relates to current stress state and loading process because granular media are anisotropic material and do not follow Hook's law. So setting up increment model can reflect the loading process better. Drucker-Prager yield criterion is a correction form of the Mohr-Coulomb yield criterion. It fits for granular media. So this paper adopts Drucker-Prager elastoplastic model in granular media simulation and finds the contact relationship between granular media and the end wall from simulated contact elements. The length of the granular media area in the model should be much more than the height of the end wall to diminish the influence of the boundary condition. The granular media area is with one free edge on the top and three other fixed edges. The boundary condition of the end wall is with one free edge on the top and three other fixed edges. Table 2 shows the material properties of the end wall and granular media. The FEM model of the end wall system was calculated by Block Lanczos law. Table 3 compares the FEM calculation result and theoretical calculation results by solving the FEM model of the end wall system according to Block Lanczos law. Taking $\delta = 0.8$, for example, Figures 9 and 10 show the first-order mode shape solved by finite element method and theoretical method.

The result shows that the nonlinear resonance frequency decreases as the height of the granular media increases. But the decreasing magnitude is not significant, and the resonant frequencies and vibration mode shapes solved by theoretical

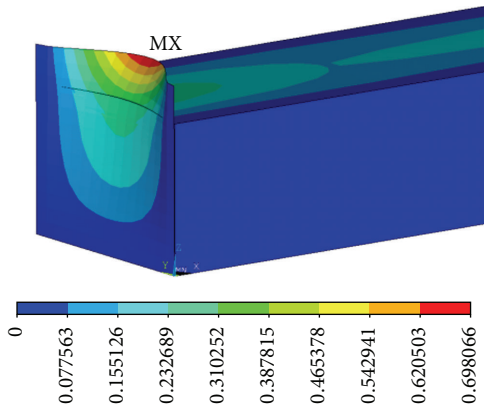

Figure 9: The first-order mode by FEM method.

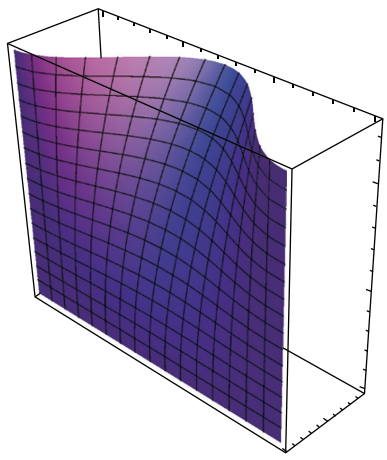

Figure 10: The first-order mode by theoretical method.

Table 2: Material properties.

Type	Density (kg/m^3)	Elastic modulus (Pa)	Poisson ratio	Cohesion (Pa)	Frictional angle (°)	Flow angle (°)
Wall	7850	2×10^{11}	0.3	—	—	—
Granular media	1636.74	2×10^{7}	0.3	0	30	15

Table 3: FEM calculation results and theoretical calculation results.

Height ratio	Theoretical calculation (Hz)	FEM calculation result (Hz)	Relative error
0	127.806	135.444	5.64%
0.4	127.782	134.786	5.20%
0.8	126.805	133.993	5.36%
1	125.767	133.499	5.79%

method and finite element method are almost the same. However, the theoretical solution is a little lower than that of FEM result. The reason is that the frequency is influenced by stiffness and quality of the system. To be more specific, the length of the granular media area is unlimited in the theoretical method, but it is limited in the finite element method. Therefore, the increment of quality makes the result lower. But the error is within acceptable range. We will discuss the influence of the finite soil volume in the theoretical model in future work. At the same time, this model provides a basis for simulating the retaining wall structure by FEM.

5. Conclusion

This paper researched the dynamics of the end wall of heavy-loading trains by theoretical methods and verified this theory by numerical simulations method. Finally, we can reach the conclusion that some key parameters are related to the design of end wall. The conclusions are as follows:

(1) In theoretical methods, this paper sets up nonlinear vibration equations which consider the affection of granular media and got the first-order approximate solution and amplitude-frequency response equations in the case of taking account of first primary resonance.

(2) It certified that the amount of materials has little effect on the nonlinear characteristics of the end wall. So whether the carriage is in working condition can be neglected.

(3) Nonlinear vibration of the structure can be minimized by setting an appropriate height-width ratio. So the optimum height-width ratio of the end wall is the key factor during the design stage of the wagon.

(4) The particle size of the granular media has little effect on the nonlinear characteristics of the structure. It is not necessary to design different carriages for different kinds of cargo.

(5) The thickness of the end wall affects the dynamics of the structure in a large part. However, it can just consider the influence of the strength instead of thickness when the thickness is greater than the particular value when studying the nonlinear characteristics.

(6) The finite element model of the end wall was established which considers the influence of the granular media. By calculating the resonant frequency under different height ratio of granular media, the result validates the correctness of the theory in the paper.

Conflict of Interests

The authors declare that there is no conflict of interests regarding the publication of this paper.

Acknowledgment

This work was financially supported by the Natural Science Foundation of Tianjin, China, Project no. 12JCZDJC28000.

References

[1] S. Argyroudis, A. M. Kaynia, and K. Pitilakis, "Development of fragility functions for geotechnical constructions: application to cantilever retaining walls," *Soil Dynamics and Earthquake Engineering*, vol. 50, pp. 106–116, 2013.

[2] M. Guaita, A. Couto, and F. Ayuga, "Numerical simulation of wall pressure during discharge of granular material from cylindrical silos with eccentric hoppers," *Biosystems Engineering*, vol. 85, no. 1, pp. 101–109, 2003.

[3] Q. Meng, J. C. Jofriet, and S. C. Negi, "Finite element analysis of bulk solids flow: part 2, application to a parametric study," *Journal of Agricultural Engineering Research*, vol. 67, no. 2, pp. 151–159, 1997.

[4] R. J. Goodey, C. J. Brown, and J. M. Rotter, "Verification of a 3-dimensional model for filling pressures in square thin-walled silos," *Engineering Structures*, vol. 25, no. 14, pp. 1773–1783, 2003.

[5] F. Ayuga, M. Guaita, and P. Aguado, "Static and dynamic silo loads using finite element models," *Journal of Agricultural Engineering Research*, vol. 78, no. 3, pp. 299–308, 2001.

[6] C. S. Zhang, Q. W. Yang, and Y. Xu, "DEM simulation to the behaviors of bulk granule within a truck body during a sudden breaking," *The Chinese Journal of Process Engineering*, vol. 2, supplement, pp. 79–83, 2002.

[7] H. He, H. Q. Tian, and F. Jiang, "Granule movement and influents to gondola car safe," in *Proceedings of the International Conference on Mechanical Engineering and Mechanics (ICMEM '07)*, pp. 1917–1921, Wuxi, China, November 2007.

[8] J. P. Wolf and D. R. Somaini, "Approximate dynamic model of embedded foundation in time domain," *Earthquake Engineering & Structural Dynamics*, vol. 14, no. 5, pp. 683–703, 1986.

[9] A. Ghanbari, E. Hoomaan, and M. Mojallal, "An analytycal method for calculating the natural frequency of retaining walls," *International Journal of Civil Engineering*, vol. 11, no. 1, pp. 1–9, 2013.

[10] K. Hatami and R. J. Bathurst, "Effect of structural design on fundamental frequency of reinforced-soil retaining walls," *Soil Dynamics and Earthquake Engineering*, vol. 19, no. 3, pp. 137–157, 2000.

[11] Y. A. Zhang, S. A. Liu, and J. G. Chen, "Influence and its application of soil on the mode of cantilever retaining wall," *Journal of Civil, Architectural & Environmental Engineering*, vol. 31, no. 3, pp. 72–77, 2009.

[12] L. B. Liu, Y. X. Zhang, and J. G. Chen, "Dynamic-detection model of soil-wall system and the identification method of virtual parameter," *Journal of Northwest A & F University (Natural Science Edition)*, vol. 40, no. 10, pp. 223–227, 2012.

[13] G. X. Cao, *Vibration of Thin Rectangular Elastic Plate*, China Building Industry Press, Beijing, China, 1983.

[14] F. Q. Liu, "Lateral earth pressures acting on circular retaining walls," *International Journal of Geomechanics*, vol. 14, no. 3, 2014.

[15] T. Tanchaisawat, D. T. Bergado, and P. Voottipruex, "Numerical simulation and sensitivity analyses of full-scale test embankment with reinforced lightweight geomaterials on soft Bangkok clay," *Geotextiles and Geomembranes*, vol. 26, no. 6, pp. 498–511, 2008.

[16] A. Kitsabunnarat, M. Alsaleh, and S. Helwany, "Capturing strain localization in reinforced soils," *Acta Geotechnica*, vol. 3, no. 3, pp. 175–190, 2008.

[17] S.-Y. Hsia and Y.-T. Chou, "Traffic noise propagating from vibration of railway wagon," *Mathematical Problems in Engineering*, vol. 2013, Article ID 651797, 7 pages, 2013.

[18] X.-H. Bao, G.-L. Ye, B. Ye, Y. Sago, and F. Zhang, "Seismic performance of SSPQ retaining wall-centrifuge model tests and numerical evaluation," *Soil Dynamics and Earthquake Engineering*, vol. 61-62, pp. 63–82, 2014.

[19] F. Zhang, B. Ye, and G. L. Ye, "Unified description of sand behavior," *Frontiers of Architecture and Civil Engineering in China*, vol. 5, no. 2, pp. 121–150, 2011.

[20] A. Athanasopoulos -Zekkos, V. S. Vlachakis, and G. A. Athanasopoulos, "Phasing issues in the seismic response of yielding, gravity-type earth retaining walls—overview and results from a FEM study," *Soil Dynamics and Earthquake Engineering*, vol. 55, pp. 59–70, 2013.

[21] J. Q. Mao, "A finite element approach to solve contact problems in geotechnical engineering," *International Journal for Numerical and Analytical Methods in Geomechanics*, vol. 29, no. 5, pp. 525–550, 2005.

[22] X. W. Liang and Q. Liu, "Finite element analysis of the cantilever retain wall," *Journal of Huazhong University of Science and Technology (Natural Science Edition)*, vol. 20, no. 2, pp. 99–102, 2003.